Publisher Version: https://doi.org/10.1016/j.jinorgbio.2015.11.028

Cytotoxicity-boosting of kiteplatin by Pt(IV) prodrugs with axial benzoate ligands.

Nicola Margiotta,[1,] Salvatore Savino,[1] Cristina Marzano,[2] Concetta Pacifico,[1] James D. Hoeschele,[3] Valentina Gandin,[2] Giovanni Natile.[1,*]*

[1]Dipartimento di Chimica, Università degli Studi di Bari Aldo Moro, via E. Orabona 4, 70125 Bari (Italy);

[2]Dipartimento di Scienze del Farmaco, Università di Padova, via Marzolo 5, 35131 Padova (Italy);

[3]Department of Chemistry, Eastern Michigan University, Ypsilanti, MI, USA 48197.

HIGHLIGHTS

- Two new Pt(IV) lipophilic prodrugs of kiteplatin have been synthesized and characterized.
- The benzoate axial ligands do increase the uptake of the two prodrugs.
- The cytotoxicity of the compounds has shown that they are active at nanomolar concentration.
- The benzoate Pt(IV) prodrugs are also able to overcome cisplatin- and oxaliplatin-resistance.

Cytotoxicity-boosting of kiteplatin by Pt(IV) prodrugs with axial benzoate ligands.

Nicola Margiotta,[1,*] *Salvatore Savino,*[1] *Cristina Marzano,*[2] *Concetta Pacifico,*[1] *James D. Hoeschele,*[3] *Valentina Gandin,*[2] *Giovanni Natile.*[1,*]

[1]Dipartimento di Chimica, Università degli Studi di Bari Aldo Moro, via E. Orabona 4, 70125 Bari (Italy);

[2]Dipartimento di Scienze del Farmaco, Università di Padova, via Marzolo 5, 35131 Padova (Italy);

[3]Department of Chemistry, Eastern Michigan University, Ypsilanti, MI, USA 48197.

Keywords: Kiteplatin; Pt(IV) complexes; benzoate ligands; cellular accumulation; cell growth inhibition; X-ray crystal structure.

Abstract

Kiteplatin, the neglected drug analogous of cisplatin but containing *cis*-1,4-DACH in place of the two ammines, has been recently reevaluated for its activity against cisplatin- and oxaliplatin-resistant tumors, in particular colo-rectal cancer. With the aim of further improving the pharmacological activity of this drug, Pt(IV) prodrugs were derived by addition of two, differently substituted, benzoate groups in axial positions (X-ray structure). The cytotoxic activity of both compounds resulted markedly potentiated reaching nanomolar concentration against a wide panel of human cancer cells. The ability of benzoate ligands to enhance the activity of kiteplatin most likely originates from their lipophilicity promoting a higher drug accumulation in cancer cells; however, it

[*] **Corresponding Authors:** Phone: +39 080 5442759 (N.M.); +39 080 5442774 (G.N.). E-mail: nicola.margiotta@uniba.it (N.M.); giovanni.natile@uniba.it (G.N.).

is to be noted that the increase in pharmacological effect is far greater than the increase in cellular uptake. The overcome of cisplatin- and oxaliplatin-resistance in the case of kiteplatin derivatives appears to depend upon inability of membrane extrusion pumps to remove Pt active species from tumor cells.

1. Introduction

Platinum(II) based drugs, such as cisplatin, carboplatin and oxaliplatin (Chart 1) are the first line treatment for many types of malignancies, including testicular, ovarian and lung cancer.[1,2] The most generally accepted mode of action of cisplatin contemplates its binding to DNA and failure of repair mechanisms to remove Pt-DNA adducts ultimately triggering apoptotic cellular suicide.[3-5] A valuable new candidate platinum anticancer drug is [$PtCl_2$(*cis*-1,4-DACH)] (DACH = diaminocyclohexane), also named kiteplatin (Chart 1), that contains an isomeric form of the diamine ligand (1*R*,2*R*-DACH) found in oxaliplatin. In particular, the interest in this compound stems from its activity against cisplatin (2008/C13* ovarian cancer cells) and oxaliplatin (LoVo/LoVo-OXP colon cancer cells) sensitive and resistant cell lines. The cross-resistance profiles indicate that kiteplatin is at least as good as oxaliplatin and significantly better than cisplatin (particularly in the case of colon cancer cells) toward the sensitive sublines. Furthermore, despite sharing similar lipophilicity values with oxaliplatin and a similar propensity for passive diffusion, the accumulation of kiteplatin is not reduced in oxaliplatin-resistant cells lines. In addition, the 1,2-GG intrastrand crosslinks formed by [$PtCl_2$(*cis*-1,4-DACH)] inhibit DNA polymerase more efficiently than the analogous adducts formed by cisplatin, potentiating the activity of this complex.[6-8]

Chart 1 here.

Also in the case of platinum, the synthesis of prodrugs has been exploited to mitigate the limitations of conventional platinum(II) anticancer complexes. An early example has been the platinum(IV) derivative satraplatin (Chart 2) currently undergoing Phase III clinical trials.[9] The Pt(IV) complexes, with their two additional coordination sites, also offer greater synthetic flexibility and the possibility to prepare drugs for oral administration. For instance, Lippard et al. have demonstrated that a Pt(IV)-estrogen complex (Chart 2), containing two estrogen derivatives linked, via a succinate moiety, to axial positions of Pt(IV) substrate, was able to sensitize estrogen-receptor(+) mammalian tumor cells to platinum treatment.[10] Similarly, the group of Dyson has shown that a Pt(IV)-ethacrynic acid complex can inhibit the activity of glutathione-S-transferase, a multidrug resistance enzyme, in vitro.[11] Therefore, the *trans*-Pt(IV) carboxylate moiety represents a versatile framework for the incorporation of functional groups into platinum-based compounds.[10] The *trans*-Pt(IV) carboxylates can be rapidly reduced, under physiological conditions, by biological reducing agents, such as glutathione and ascorbic acid, to release the functionalized ligands and the cytotoxic Pt(II) species.[12] In addition, the axial ligands can be exploited to modulate the lipophilic character of Pt(IV) complexes. Aryl groups have been shown to improve the uptake of drugs by conferring greater lipophilicity and facilitating transport across the cell membrane. For example, it has been found that aryl ethers of functionalized glycomers are effective cell growth inhibitors and induce apoptosis in human glioblastoma cells.[13]

Benzoate axial ligands were first introduced by Dyson and Ang.[11,14,15] Ang demonstrated that a dibenzoate Pt(IV) derivative of cisplatin was 30-fold more cytotoxic than cisplatin in the A2780 human ovarian carcinoma cell line. However, this compound was not able to overcome cisplatin-resistance in the A2780/CisR cell line.[14] Dyson also explored the role of para substituents (including vinyl-, methoxy-, iodo-, and cyano- groups) to modulate the lipophilicity of *cis*,*trans*,*cis*-$[PtCl_2(benzoate)_2(NH_3)_2]$ compounds (Chart 2). A strong relationship was found between drug efficacy and uptake and between complex accumulation and lipophilicity of the benzoic ligands

present in the complex, the complexes with *para*-vinyl-benzoate and *para*-methoxy-benzoate showing the highest cellular uptake.[15]

In a recent work, some of us demonstrated that it is possible to overcome the oxaliplatin-resistance in colorectal cancer cells by exploiting the high lipophilicity of the Pt(IV) oxaliplatin prodrug *cis*,*trans*,*cis*-[$PtCl_2$(benzoate)$_2$(1*R*,2*R*-DACH)] (Chart 2). This latter compound showed a better *in vitro* antiproliferative activity than oxaliplatin and was active also in the LoVo-OXP cell line.[16]

Chart 2 here.

With the aim of improving the drug uptake and, hence, the pharmacological activity of kiteplatin in cancer cells, we have prepared two new Pt(IV) prodrugs of kiteplatin having different aryl groups in axial positions: *cis*,*trans*,*cis*-[$PtCl_2$(benzoate)$_2$(*cis*-1,4-DACH)] (**1** in Scheme 1) and *cis*,*trans*,*cis*-[$PtCl_2$(3,4,5-trimethoxybenzoate)$_2$(*cis*-1,4-DACH)] (**2** in Scheme 1).

The two new complexes have been characterized and tested *in vitro* against a panel of human cancer cells, either sensitive or resistant to platinum drugs, by means of cytotoxicity and cell growth recovery studies. In addition, cellular uptake experiments were performed in order to correlate the cytotoxicity of the new derivatives with their uptake by tumor cells.

2. Experimental Section

2.1 Materials and methods.

Commercial reagent grade chemicals and solvents were used as received without further purification. ^{1}H-NMR, ^{195}Pt-NMR and [^{1}H-^{195}Pt] HSQC spectra were recorded on a Bruker Avance DPX 300 MHz instrument. [^{1}H-^{13}C]-HSQC spectra were recorded on a Bruker Avance III 700 MHz instrument. ^{1}H and ^{13}C chemical shifts were referenced using the internal residual peak of the solvent (DMSO-d_6: 2.50 ppm for ^{1}H and 39.51 ppm for ^{13}C). ^{195}Pt NMR spectra were referenced to K_2PtCl_4 (external standard placed at -1620 ppm with respect to $Na_2[PtCl_6]$).[17]

Electrospray ionisation mass spectrometry (ESI-MS) was performed with an electrospray interface and an ion trap mass spectrometer (1100 Series LC/MSD Trap system Agilent, Palo Alto, CA). Elemental analyses were carried out with an Eurovector EA 3000 CHN instrument. The Fourier transform infrared spectra were obtained on a Perkin Elmer Spectrum One instrument, using KBr pellets, in the range 4000-200 cm^{-1}. Intensities of the reported bands are described with s for strong, m for medium and w for weak; broad signals are additionally specified with letter b in front of these abbreviations.

Kiteplatin[18] and *cis,trans,cis*-[$PtCl_2(OH)_2$(*cis*-1,4-DACH)][19] (compound **3**) were prepared according to already reported procedures and the given formulation was in good agreement with analytical values (data not shown).

2.2 Synthesis of *cis,trans,cis*-[$PtCl_2$(benzoate)$_2$(*cis*-1,4-DACH)] (**1**). Compound **1** was prepared by adapting already reported procedures.[11,16] A solution of benzoyl chloride (1.42 mL, 12.18 mmol) in 8 mL of acetone was added dropwise to a mixture of *cis,trans,cis*-[$PtCl_2(OH)_2$(*cis*-1,4-DACH)] (194.1 mg, 0.47 mmol) and pyridine (1.56 mL, 19.31 mmol) in acetone (4 mL). The reaction mixture was stirred at reflux for 4 h in the dark. After cooling the suspension to room temperature, the resulting white precipitate was eliminated by filtration. An excess of n-pentane was added to the filtrate to yield a pale yellow precipitate that was isolated by filtration of the mother liquor. The obtained solid was redissolved in THF, precipitated with n-pentane, washed with water and diethyl ether, and dried under vacuum (yield 60%; 180 mg).

Anal.: calculated for $C_{20}H_{24}Cl_2N_2O_4Pt$·1/4diethyl ether (**1**·1/4 $C_4H_{10}O$): C, 39.35; H, 4.17; N, 4.37 %. *Found*: C, 39.63; H, 4.02; N, 4.60 %. ESI-MS: *calculated for* $C_{20}H_{24}Cl_2N_2O_4PtK$, [**1** + K]$^+$: 661.03. *Found :* $^m/_z$ 661.10. ^{1}H NMR (DMSO-d_6): 8.37 (4H, NH_2), 8.00 (4H, C*Ho*), 7.57 (2H, C*Hp*), 7.47 (4H, C*Hm*), 3.09 (2H, C*Ha*), 1.64 (8H, C*Hb,c*) ppm. ^{13}C NMR (DMSO-d_6): 20.0 (*CHb,c*), 49.8 (*CHa*), 127.8 (*CHm*), 129.3 (*CHo*), and 132.0 (*CHp*) ppm (see Scheme 1 for numbering of atoms). ^{195}Pt NMR (DMSO-d_6): 1176.2 ppm. FT-IR: ν = 3249 bm (ν_{N-H}), 3067 bm

(ν_{N-H}), 2944 w (ν_{C-H}), 1633 s ($\nu_{as\ C=O}$), 1533 m ($\nu_{as\ C=O}$), 1318 s, 1297 s, 1241 m, 1129 m, 337 w (ν_{Pt-Cl}). Crystals suitable for X-ray analysis were obtained by slow evaporation of a solution of **1**·1/4 $C_4H_{10}O$ in acetone.

2.3 Synthesis of *cis,trans,cis*-[$PtCl_2$(3,4,5-trimethoxybenzoate)$_2$(*cis*-1,4-DACH)] (2). A solution of 3,4,5-trimethoxybenzoyl chloride (1.303 g, 5.65 mmol) in 20 mL of $CHCl_3$ was added dropwise to a suspension of *cis,trans,cis*-[$PtCl_2(OH)_2$(*cis*-1,4-DACH)] (90 mg, 0.22 mmol) and pyridine (724 μL, 8.95 mmol) in 10 mL of $CHCl_3$. The mixture was refluxed for 4 h and left under stirring at room temperature for further 16 h in the dark. The reaction mixture was filtered and an excess of n-pentane was added to the filtrate to yield a yellow precipitate that was isolated by filtration of the mother liquor. The precipitate was washed with water and 2 mL of THF, then redissolved in $CHCl_3$ and precipitated by addition of pentane. The isolated product was dried under vacuum (yield 30%; 55 mg). *Anal.: calculated for* $C_{26}H_{36}Cl_2N_2O_{10}Pt\cdot 2H_2O$ (**2**·$2H_2O$): C, 37.24; H, 4.81; N, 3.34 %. *Found*: C, 37.10; H, 4.39; N, 3.54 %. ESI-MS: *calculated for* $C_{26}H_{36}Cl_2N_2O_{10}PtNa$, [**2** + Na]$^+$: 825.12. *Found :* $^m/_z$ 825.10. ^{1}H NMR (DMSO-d_6): 8.37 (4H, N*H*$_2$), 7.31 (4H, C*Ho*), 3.83 (12H, C*H*$_3$*m*), 3.72 (6H, C*H*$_3$*p*), 3.1 (2H, C*Ha*), 1.65 (8H, C*Hb,c*) ppm. ^{195}Pt NMR (DMSO-d_6): 1177.5 ppm. ^{13}C NMR (DMSO-d_6): 19.8 (*C*H*b,c*), 49.67 (*C*H*a*), 55.8 (*C*H$_3$*m*), 60.0 (*C*H$_3$*p*), and 107.0 (*C*H*o*) ppm (see Scheme 1 for numbering of atoms). FT-IR: ν = 3219 bm (ν_{N-H}), 2940 w (ν_{C-H}), 1624 m ($\nu_{as\ C=O}$), 1586 m ($\nu_{as\ C=O}$), 1333 s, 1275 m, 1230 m, 1125 s, 331 w (ν_{Pt-Cl}).

2.4 X-ray Crystallography.

A selected crystal of **1** was mounted on a Bruker AXS X8 APEX CCD system equipped with a four-circle Kappa goniometer and a 4K CCD detector (radiation Mo Kα). For data reduction and unit cell refinement, the SAINT-IRIX package was employed.[20] A total of 10925 reflections with Θ_{max} = 23.54 (a low value for Θ_{max} was used because the crystals resulted to be sensitive to X-rays

and decomposed for prolonged irradiation) were collected, indexed, integrated, and corrected for Lorentz, polarization, and absorption effects using the program SADABS.[21] The unit cell dimensions were calculated from all reflections, and the structure was solved using the direct methods technique in the $C_{2/c}$ space group. The model was refined by full-matrix least-squares methods. All non-hydrogen atoms were refined anisotropically. All hydrogen atoms were placed at calculated positions and refined given isotropic parameters equivalent to 1.2 times those of the atom to which they are attached. All calculations and molecular graphics were carried out using SIR2004,[22] SHELXL97,[23] PARST97,[24,25] WinGX,[26] and ORTEP-3[27] for Windows packages. Details of the crystal data are listed in Table 1. Selected bond lengths and angles are listed in Table 2.

Crystallographic data (without structure factors) have been deposited with the Cambridge Crystallographic Data Centre as supplementary publication no. CCDC 1426597. Copies of the data can be obtained free of charge from the CCDC (12 Union Road, Cambridge CB2 1EZ, UK; phone, (+44) 1223−336−408; fax, (+44) 1223−336−003; e-mail, deposit@ccdc.cam.ac.uk; Web site http://www.ccdc.cam.ac.uk/data_request/).

2.5 Stability of *cis,trans,cis*-[$PtCl_2$(benzoate)$_2$(*cis*-1,4-DACH)] (1)

150 μL of a solution of **1** (0.8 mM) in DMSO was diluted to 3.0 mL with standard physiological saline solution (0.9 %, w/v; pH = 6.2) to obtain a final concentration of 40 μM of complex **1** in saline solution. The mixture was incubated at 37 °C in the dark and the hydrolysis reaction was followed by monitoring the decrease of the chromatographic peak of the starting Pt(IV) complex by HPLC-UV. Stationary phase: Waters Symmetry RP-C18 column, 5 μM, 4.6 × 250 mm, 100 Å. Mobile phase: phase A = water and phase B = Acetonitrile; isocratic elution 5% phase B for 5 min, linear gradient from 5% to 20% phase B in 6.5 min, isocratic elution 20% phase B for 5.5 min, linear gradient from 20% to 100% phase B in 10 min, isocratic elution 100% phase B for 5 min,

linear gradient from 100% to 5% phase B in 1 min, isocratic elution 5% phase B for 10 min. Flow rate = 0.6 mL min^{-1}. UV-visible detector set at 220 nm.

2.6 Experiments with cultured human cells.

Pt(IV) compounds **1** and **2** and their dihydroxido precursor *cis,trans,cis*-[$PtCl_2(OH)_2$(*cis*-1,4-DACH)] (**3**) were dissolved in DMSO just before the experiment and a calculated amount of drug solution was added to the cell growth medium to a final solvent concentration of 0.5% (a percentage of DMSO that has no detectable effect on cell killing). Cisplatin (Sigma Chemical Co.) and kiteplatin were dissolved in 0.9% NaCl solution.

2.6.1 Cell cultures.

Human breast (MCF-7), colon (HCT-15 and LoVo), lung (A549), and pancreatic (BxPC3) carcinoma cell lines along with melanoma (A375) cells were obtained from American Type Culture Collection (ATCC, Rockville, MD). The human ovarian cancer cell line 2008 and its cisplatin resistant variant, C13*, were kindly provided by Prof. G. Marverti (Dept. of Biomedical Science of Modena University, Italy). The human colon carcinoma LoVo-OXP cells were derived, using a standard protocol, by growing LoVo cells in increasing concentrations of oxaliplatin and following 17 months of selection of resistant clones, as previously described.[28] Cell lines were maintained in the logarithmic phase at 37 °C in a 5% carbon dioxide atmosphere using the following culture media containing 10% fetal calf serum (Euroclone, Milan, Italy), antibiotics (50 units/mL penicillin and 50 μg/mL streptomycin) and 2 mM L-glutamine: (i) RPMI-1640 medium (Euroclone) for 2008, C13*, MCF-7, HCT-15 and BxPC3 cells; (ii) F-12 HAM'S (Sigma Chemical Co.) for A549, LoVo and LoVo-OXP cells; iii) DMEM (Sigma Chemical Co.) for A375 cells.

2.6.2 Cytotoxicity assays.

The growth inhibitory effect toward tumor cells was evaluated by means of the MTT assay. Briefly, (3 - 8) x 10^3 cells/well, depending upon the growth characteristics of the cell line, were seeded in 96-well microplates in growth medium (100 μL). After 24 h, the medium was removed and replaced with fresh medium containing the compound to be studied at the appropriate concentration. Triplicate cultures were established for each treatment. After 72 h, each well was treated with 10 μL of a 5 mg/mL MTT saline solution and, following 5 h of incubation, 100 μL of a sodium dodecylsulfate (SDS) solution in 0.01 M HCl were added. After an overnight incubation, cell growth inhibition was detected by measuring the absorbance of each well at 570 nm using a Bio-Rad 680 microplate reader. The mean absorbance for each drug dose was expressed as a percentage of the absorbance of the control untreated well and plotted vs drug concentration. Data were fitted to a dose–response curve and IC_{50} values, the drug concentration that decreases the mean absorbance at 570 nm to 50% that of untreated cells control wells, were calculated with the four-parameter logistic model (4PL). The final value is the mean ± S.D. of at least three independent experiments performed in triplicate.

In the cell growth recovery experiments, after 6 h of treatment at the indicated concentrations, the drug-containing medium was replaced with a fresh complete medium, which was maintained for additional 66 h before MTT determination.

2.6.3 Cellular uptake.

LoVo cells ($2 \cdot 10^6$) were seeded in 75 cm^2 flasks in growth medium (20 mL). After 24 h, the medium was replaced and the cells incubated for 24 h in the presence of the tested complexes. Cell monolayers were washed twice with cold PBS and harvested. Samples were subjected to three freeze/thaw cycles at −80 °C, and then vigorously vortexed. Aliquots were removed for the determination of protein content by the Bradford protein assay (BioRad). The samples were treated with 1 mL of highly pure nitric acid (Pt: ≤ 0.01 $mg \cdot kg^{-1}$, TraceSELECT Ultra, Sigma Chemical Co.) and transferred into a microwave Teflon vessel. Subsequently, samples were submitted to standard

procedure using a speed wave MWS-3 Berghof instrument (Eningen, Germany). After cooling, each mineralized sample was analyzed for platinum by using a Varian AA Duo graphite furnace atomic absorption spectrometer (Varian, Palo Alto, CA, USA) at λ 324.7 nm. The calibration curve was obtained using known concentrations of standard solutions purchased from Sigma Chemical Co.

3. Results and Discussion

3.1 Synthesis and characterization of 1 and 2

The balance between lipophilicity and water solubility of a drug plays a key role in its bioavailability, therefore we decided to increase the lipophilicity of Pt(IV) derivatives of kiteplatin by coordinating benzoate and 3,4,5-trimethoxybenzoate in axial positions. Compounds **1** and **2** were synthesized by acylation of the dihydroxido platinum(IV) precursor *cis,trans,cis*-[$PtCl_2(OH)_2$(*cis*-1,4-DACH)] (**3**) with benzoyl chloride or 3,4,5-trimethoxybenzoyl chloride (Scheme 1). The reactions were carried on in the presence of pyridine to neutralize the released HCl and in the dark to avoid the possible spontaneous solvent-assisted reduction of **3** to kiteplatin.[11,16,19,29] Better yields were obtained performing the reaction in acetone in the case of compound **1** and in $CHCl_3$ in the case of **2**.

Scheme 1 here.

The ESI-MS spectrum of **1** showed the presence of a peak at *m/z* = 661.10 corresponding to $[\mathbf{1}+K]^+$ as also confirmed by the isotopic pattern (data not shown).

The ^1H NMR spectrum of **1** in DMSO-d_6 is reported in Figure S1 (top) in the Supplementary Information (SI). The singlet with Pt satellites falling at 8.37 ppm ($^2J_{H\text{-}Pt}$= 62.47 Hz) was assigned to the aminic protons of coordinated *cis*-1,4-DACH. The doublet falling at 8.00 ppm ($^3J_{H\text{-}H}$= 6.82 Hz) was assigned to the *ortho* protons of carboxylate groups (H*o* in Scheme 1), while the multiplets located at 7.57 and 7.47 ppm were assigned, respectively, to the *para* and the *meta* protons of coordinated benzoates (H*p* and H*m* in Scheme 1). The singlet with Pt satellites ($^3J_{H\text{-}Pt}$= 78.0 Hz) at

3.09 ppm and the multiplet integrating for eight protons detected at 1.64 ppm were assigned, respectively, to the methinic and methylenic groups of coordinated DACH.

The [^{1}H-^{195}Pt]-HSQC 2D NMR spectrum recorded on compound **1** dissolved in DMSO-d_6 is reported in Figure S1 (bottom; SI). The spectrum shows two cross peaks falling at 8.37/1176.2 and 3.09/1176.2 ppm (^{1}H/^{195}Pt). The ^{195}Pt chemical shift is at lower field with respect to that of the precursor compound **3** (964.6 ppm in DMSO-d_6)[19] and in good agreement with that already reported for similar Pt(IV) aryl carboxylate derivatives such as *cis,trans,cis*-[$PtCl_2$(benzoate)$_2$(NH_3)$_2$] (1076.63 ppm in THF-d_8).[15]

The [^{1}H-^{13}C] HSQC 2D spectrum of complex **1** in DMSO-d_6 (Figure S2, bottom; SI) showed a cross peak correlating the ^{1}H signal of the methinic protons of coordinated DACH with a ^{13}C signal at 49.8 ppm and a cross peak correlating the ^{1}H signal of the methylenic protons of DACH with a ^{13}C signal at 20.0 ppm. The *ortho, para* and *meta* carbon atoms of coordinated benzoates resonate at 129.3, 132.0, and 127.8 ppm, respectively, in good agreement with literature data for *cis,trans,cis*-[$PtCl_2$(benzoate)$_2$(*1R,2R*-DACH)] (131.2, 133.5, and 129.2 ppm, in CD_3OD).[16]

The ESI-MS spectrum of **2** showed the presence of a peak at *m/z* = 825.10 corresponding to [**2** + Na]$^{+}$ (theoretical *m/z* = 825.12). The ^{1}H NMR of **2** in DMSO-d_6 is reported in Figure S3 (top; SI). The singlet with Pt satellites detected at 8.37 ppm ($^{2}J_{H\text{-}Pt}$ = 61.72 Hz) was assigned to the aminic protons of coordinated *cis*-1,4-DACH. The singlet observed at 7.31 ppm was assigned to the aromatic protons in *ortho* position to the carboxylato group (H*o* in Scheme 1). The two singlets falling at 3.83 and 3.72 ppm were assigned to the methoxy groups in *meta* and *para* positions, respectively. The singlet located at. 3.10 and 1.65 ppm were assigned to the methinic and methylenic protons of *cis*-1,4 DACH, respectively.

The NMR characterization of carbon atoms was obtained by a [^{1}H-^{13}C]-HSQC 2D NMR experiment performed in DMSO-d_6 (Figure S3, bottom; SI). The cross peaks at 3.10/49.67 and 1.65/19.8 ppm (^{1}H/^{13}C) were assigned to the methinic and methylenic groups of DACH,

respectively. The *ortho* carbon atoms of coordinated 3,4,5-trimethoxybenzoate fall at 107.0 ppm, and are more shielded than the corresponding carbon atoms in compound **1**. This behaviour is probably due to the positive mesomeric effect of the methoxy groups of the aryl rings. Finally the cross peaks detected at 3.83/55.8 and 3.72/60.0 ppm ($^{1}H/^{13}C$) were assigned to the $–OCH_3$ groups in *meta* and in *para* positions. These values are quite similar to that found by Dyson for the methoxy groups of *cis*,*trans*,*cis*-[$PtCl_2$(4-methoxybenzoate)$_2$(NH_3)$_2$] (55.6 ppm).

The ^{195}Pt NMR of **2** in DMSO-d_6 is reported in Figure S4. It shows a broad singlet observed at 1177.5 ppm, a chemical shift similar to that of **1**.

3.2 X-ray characterization of compound 1.

The asymmetric unit comprises half molecule of *cis*,*trans*,*cis*-[$PtCl_2$(benzoate)$_2$(*cis*-1,4-DACH)] and the overall structure is generated by a two-fold axis parallel to the *b* axis and passing through the Pt atom (Figure 1).

Figure 1 here.

Two equatorial positions are occupied by the nitrogen atoms of 1,4-DACH while the other two positions are occupied by chlorides. The axial positions are occupied by oxygen atoms of benzoate ligands. The Pt1─N1, Pt1─O1, and Pt1─Cl1 bond lengths are within the range normally observed for platinum(II) and platinum(IV) complexes (Table 2).

The DACH ligand is in a twist-boat configuration with a N1-Pt1-N1(-*x*+1,+*y*,-*z*+1/2+1) angle of 96.8(4)° and the C8–N1–Pt1 angle of 124.5(6)°. In compensation for the large bite angle of coordinated *cis*-1,4-DACH, the N1-Pt-Cl1 bond angle is reduced to 86.1(2)°. Large N–Pt–N and C–N–Pt angles are a common feature of complexes with *cis*-1,4-DACH-Pt, such as [$PtCl_4$(*cis*-1,4-DACH)],[30] *cis*,*trans*,*cis*-[$PtCl_2$(acetate)$_2$(*cis*-1,4-DACH)],[31] and *cis*,*trans*,*cis*-[Pt(*cis*-1,4-DACH)Cl_2(1,1-cyclobutanedicarboxylato)].[32]

The carboxylic group is coplanar to the aromatic ring indicating the presence of an extensive electron delocalization. Strong intramolecular hydrogen bonds link the aminic groups with the

benzoate ligands (N1—H1a···O2) (Figure 1 and Table 3), while intermolecular H-bonds link aminic groups and benzoate ligand of adjacent molecules (N1—H1b···$O2^{i}$, i=-x+1,-y+1,-z+2) (Table 3). These intermolecular interactions allow the formation of chains that extend along the *c* axis. Intermolecular hydrogen bonds are also formed between DACH C–H and chlorine atoms (C10—H10a···$Cl1^{ii}$, ii= -x+1,+y+1,-z+1/2+1), these latter allow formation of chains extending along the *b* axis (Figure 2, Table 3).

Figure 2 here.

3.3 Stability of compound 1 in saline.

Pt(IV) prodrugs are generally assumed to escape degradation by nucleophiles in the blood and to reach the tumor intact. Once inside the cells, Pt(IV) prodrugs can be activated by reduction thereby releasing the cytotoxic Pt(II) species and the two axial ligands.[12,33,34] However, this is not always true, for instance Pt(IV) complexes with haloacetato ligands in the axial positions have been shown to undergo rather fast hydrolysis under biologically relevant conditions with release of two molecules of haloacetate and formation of a Pt(IV) dihydroxido species. Hence, HPLC analysis of water solutions (pH 7, 37 °C) of [Pt(OXA)$(TFA)_2$(*1R,2R*-DACH)] (TFA = trifluoroacetate; OXA = oxalate), [Pt(OXA)$(DCA)_2$(*1R,2R*-DACH)] (DCA = dichloroacetate) and *cis,trans,cis*-[$PtCl_2(DCA)_2(NH_3)_2$] (mitaplatin)[35] revealed that these compounds undergo hydrolysis with half lives of 6, 180, and 120 minutes, respectively,[36] a rather short time if compared to the 24-96 hours incubation times usually used in *in vitro* cytotoxicity studies. However, notwithstanding these compounds are likely to undergo hydrolysis in the extracellular medium of the cancer cells, both [Pt(OXA)$(TFA)_2$(*1R,2R*-DACH)][37] and mitaplatin proved to be very active in a variety of cancer cell lines.

Also Pt(IV) derivative of kiteplatin with dichloroacetate ligands (*cis,trans,cis*-[$PtCl_2(DCA)_2$(*cis*-1,4-DACH)] was found to undergo quite rapid degradation with a first order kinetic (half-life, $t_{1/2}$, of 28.7 min; N. Margiotta, S. Savino, V. Gandin, J. D. Hoeschele, C. Marzano, G. Natile, (2015)

submitted). Moreover, we observed that *cis,trans,cis*-[$PtCl_2(DCA)_2$(*cis*-1,4-DACH)] undergoes, simultaneously to hydrolysis, also spontaneous reduction to platinum(II) as already observed for Pt(IV) derivatives of kiteplatin in solvents such as DMSO or DMF.[19]

In order to check if Pt(IV) derivatives of kiteplatin with axial benzoate ligands also undergo hydrolysis, complex **1** was dissolved in unbuffered saline at pH = 6.2 and the area of its HPLC peak monitored as a function of time. Because of the poor solubility of **1** in water, the complex was first dissolved in DMSO and then diluted in physiological saline solution (pH = 6.2) to obtain a DMSO/saline mixture of 5:95, V/V. The HPLC chromatograms, taken at different times of incubation (37 °C, in the dark), are reported in Figure 3.

The starting material, **1**, (peak A in Figure 3 with a retention time, R.T., of 30.5 minutes) was transformed with time into a new species (peak B) having R.T. of 28.2 min. The new species B can be confidently assigned to free benzoic acid by comparison with pure benzoic acid analyzed in the same experimental conditions (data not shown; see also Scheme 2).

Scheme 2 here.

Another peak (C; R.T. = 29.2 min) was clearly visible in the chromatogram taken after 24 h incubation. This peak, together with peak B, increased in intensity over time. After 78.5 hours of incubation compound **1** was present in the chromatogram with a percentage of about 20%.

Figure 3 here.

Unfortunately, the completely hydrolyzed species **3** and kiteplatin have the same retention time of DMSO (N. Margiotta, S. Savino, V. Gandin, J. D. Hoeschele, C. Marzano, G. Natile, (2015) submitted), which gives a very strong and large peak in the chromatogram at R.T. of 4.6-10 min. Other peaks were also present in the chromatogram (*e.g.* peak having R.T. of ca. 17 min). We tentatively assign peak C to the product of first hydrolysis which could be in equilibrium with the starting complex (**1**) and the end hydrolysis product **3**.

The HPLC investigation has shown that the degradation of **1** is quite slow and follows a first order kinetic ($A_t = A_0 \exp^{-kt}$ where A_t = area of peak A at time t, A_0 = area of peak A at t = 0, and k = rate

constant). The computed value of k was 1.60 min^{-1} (Figure S5 in the SI), corresponding to a half-life ($t_{1/2}$) of 25.9 h.

3.4 Cytotoxicity studies.

The *in vitro* antitumor activity of the Pt(IV) complexes **1** and **2** was evaluated on a panel of human cancer cell lines and compared to that of cisplatin, kiteplatin, and the precursor *cis,trans,cis*-[$PtCl_2(OH)_2$(*cis*-1,4-DACH)] (**3**). Cell lines representative of colon (HCT-15), lung (A549), breast (MCF-7) and pancreatic (BxPC3) carcinoma as well as melanoma (A375) have been included. Cytotoxicity was evaluated by means of the MTT test after 72 h of treatment with increasing concentrations of the compounds. IC_{50} values, calculated from dose-survival curves, are reported in Table 4.

Compounds **1** and **2** were found to be much more effective than the reference compound cisplatin (CDDP). In particular, complex **1** showed antitumor activity already at nanomolar concentrations, being roughly two order of magnitude more active than CDDP towards all tested cell lines (average IC_{50} = 0.06 and 8.4 μM for **1** and CDDP, respectively). Compound **2** was less active than **1** by a factor of 6 but still more active than cisplatin by a factor of 24 (average IC_{50} = 0.4 and 8.4 μM for **2** and CDDP, respectively). Moreover, both complexes **1** and **2** were more effective by a factor of 340 and 51, respectively, than their Pt(IV) precursor **3** (average IC_{50} = 20.4 μM).

The lipophilic compounds **1** and **2** also possess a mean cytotoxic potency higher than that of kiteplatin (average IC_{50} = 2.7 μM) which is the released product after reduction in the tumor cell.

The effect of the am(m)ine ligands can be sized by comparing the present data with those of the analogous compounds with benzoate ligand derived from cisplatin or oxaliplatin.[15,16] The antitumor activity of *cis,trans,cis*[$PtCl_2(benzoate)_2(NH_3)_2$] against A549 cells (tested in identical experimental conditions as ours) was found to be 31 times smaller than that of compound **1**;[15]

however, the activity of *cis,trans,cis*-[$PtCl_2$(benzoate)$_2$(1*R*,2*R*-DACH)] against the HCT-15 cell line was similar to that found for **1**.[16]

All compounds were also tested against cisplatin-sensitive and -resistant ovarian cancer cells (2008 cells and C13* cells) as well as oxaliplatin-sensitive and -resistant colon cancer cells (LoVo and LoVo-OXP). Cross–resistance profiles were evaluated by means of the resistance factor (R.F.), which is defined as the ratio between the IC_{50} value for the resistant cells and that arising from the parent cells. Both **1** and **2** exhibited no cross-resistance with cisplatin (R.F. on 2008/C13* cells of 0.7 and 0.9 for **1** and **2**, respectively, and of 10.3 for CDDP) and oxaliplatin (R.F. on LoVo/LoVo OXP cells of 0.9 and 1.6 for **1** and **2,** respectively, and of 17 for oxaliplatin[6]).

Finally, to determine whether cancer cells would resume proliferation upon removal of the Pt(IV) derivatives, we performed cell growth recovery experiments in which, after incubation with different concentrations of **1** and **2** for 6 h, the drug-containing medium was removed and replaced with fresh growth medium for additional 66h. The obtained data (Figure 4) indicate that the effect induced by **1** and **2** was not reversed upon drug withdrawal, thus suggesting the occurrence of a cytotoxic rather than a cytostatic effect.

Figure 4 here.

3.5 Cellular uptake experiments

One of the main factors determining the biological activity of a metal-based drug is its ability to cross the cell membrane and to accumulate in cancer cells. Therefore, with the aim of correlating cellular accumulation with cytotoxic activity, we investigated the cellular uptake of the platinum complexes in human LoVo colorectal cancer cells after incubation with 1 μM concentration of **1**, **2**, and **3** as well as kiteplatin. The cellular platinum content was quantified by means of graphite furnace atomic absorption spectrometry (GF-AAS) analysis, and the results, expressed as pg metal/10^6 cells, are summarized in Figure 5. All complexes exhibit an accumulation pattern that is time dependent, with the highest cell accumulation recorded after 24 h incubation. Compound **1** was

internalized by cancer cells more efficiently than **2**, and both **1** and **2** more efficiently than kiteplatin. These results correlate well with the higher cytotoxicity of compound **1** with respect to compound **2** and of **1** and **2** with respect to kiteplatin, suggesting that the hydrophobic phenyl ligands confer to benzoate Pt(IV) derivatives a higher capability to cross the cell membrane. It also appears that a relatively small increase of platinum uptake can result in a far greater cytotoxic activity.

Uptake experiments performed by treating colon cancer cells for 6 h with tested complexes and then re-incubated in fresh medium had a similar Pt content than cells solely exposed to 6 h treatment with Pt complexes. These results suggest that membrane extrusion pumps, such as those belonging to the MRP families, are not effective in washing out the platinum complexes once inside the cell.

Figure 5 here.

4. Conclusions

Inspired by the remarkable increase of activity reported for Pt(IV) complexes carrying aryl carboxylate axial ligands,[11,16] we have synthesized, characterized and tested *in vitro* two new Pt(IV) prodrugs of kiteplatin having two different aryl groups in axial positions (*cis*,*trans*,*cis*-[$PtCl_2$(benzoate)$_2$(*cis*-1,4-DACH)] (**1**) and *cis*,*trans*,*cis*-[$PtCl_2$(3,4,5-trimethoxybenzoate)$_2$(*cis*-1,4-DACH)] (**2**)) with the aim of potentiating the cytotoxic activity of kiteplatin.

The cytotoxic activity of both compounds resulted remarkably potentiated by the presence of the lipophilic axial ligands reaching nanomolar activity. Thus, compounds **1** and **2** were 45 and ca. 7 times more effective than kiteplatin.

The ability of benzoate ligands to enhance the activity of kiteplatin did not appear to depend upon the type of human tumor cell lines, therefore most likely it originates from the higher accumulation of **1** and **2** in cancer cells with respect to kiteplatin. It is noteworthy that the increase in pharmacological effect is far greater than the increase in cellular uptake.

The benzoate Pt(IV) prodrugs are also able to overcome cisplatin- and oxaliplatin-resistance probably because the membrane extrusion pumps are not effective in removing the Pt active species from the tumor cells (uptake study).

In conclusion, the unique high-and-wide antitumor activity of Pt(IV)-benzoate prodrugs of kiteplatin makes these compounds clinically attractive agents in the treatment of cancers which are also cisplatin- and oxaliplatin-resistant.

Table of Abbreviations

CDDP	cisdiaminedichloridoplatinum(II)
DACH	diaminocyclohexane
DCA	dichloroacetate
DMEM	Dulbecco's modified Eagle's medium
DMF	dimethylformamide
DMSO	dimethylsulfoxide
ESI-MS	electrospray ionisation mass spectrometry
GF-AAS	graphite furnace atomic absorption spectrometry
HSQC	heteronuclear single quantum coherence
MRP	multidrug resistant protein
MTT	(3-(4,5-Dimethylthiazol-2-yl)-2,5-Diphenyltetrazolium Bromide)
OXA	oxalate
PBS	phosphate buffer saline
RPMI	Roswell Park Memorial Institute
R.F.	Resistance Factor
R.T.	retention time
S.D.	Standard deviation
SDS	sodium dodecyl sulfate
TFA	trifluoroacetate
THF	tetrahydrofurane

Acknowledgments.

We acknowledge the University of Bari (Italy), the Italian Ministero dell'Università e della Ricerca (FIRB RINAME RBAP114AMK and PON02_00607_3621894), the Inter-University Consortium for Research on the Chemistry of Metal Ions in Biological Systems (C.I.R.C.M.S.B.), and the European Union (COST CM1105: Functional metal complexes that bind to biomolecules) for support. We are grateful to Dr. Ernesto Mesto and Prof. Emanuela Schingaro (Dipartimento di Scienze della terra e geoambientali, Università degli Studi di Bari Aldo Moro) for X-ray data collection.

Supplementary Information.

Supplementary material related to this article (Figures S1-S4: NMR spectra of compounds **1** and **2**; Figure S5: HPLC kinetic analysis) can be found online.

References

[1] L. Kelland, Nat. Rev. Cancer. 7 (2007) 573–584.

[2] M. Galanski, M. A. Jakupec, B.K. Keppler, Curr. Med. Chem., 12 (2005) 2075-2094.

[3] M.A. Fuertes, J. Castilla, C. Alonson, J.M. Perez, Curr. Med. Chem.: Anti-Cancer Agents. 2 (2002) 539-551.

[4] M. A. Fuertes, C. Alonso, J.M. Perez, Chem. Rev. 103 (2003) 645-662.

[5] W. I. Sundquist, S. J. Lippard, Coord. Chem. Rev. 100 (1990) 293-322.

[6] N. Margiotta, C. Marzano, V. Gandin, D. Osella, M. Ravera, E. Gabano, J.A. Platts, E. Petruzzella, J.D. Hoeschele, G. Natile, J. Med. Chem. 55 (2012) 7182-7192.

[7] J. Kasparkova, T. Suchankova, A. Halamikova, L. Zerzankova, O. Vrana, N. Margiotta, G. Natile, V. Brabec, Biochem. Pharmacol. 79 (2010) 552−564.

[8] V. Brabec, J. Malina, N. Margiotta, G. Natile, J. Kasparkova, Chem. Eur. J. 18 (2012) 15439-15448.

[9] C.N. Sternberg, P. Whelan, J. Hetherington, B. Paluchowska, P.H.T.J. Slee, K. Vekemans, P. Van Erps, C. Theodore, O. Koriakine, T. Oliver, D. Lebwohl, M. Debois, A. Zurlo, L. Collette. Oncology 68 (2005) 2–9.

[10] K.R. Barnes, A. Kutikov, S. J. Lippard, Chem. Biol. 11 (2004) 557-564.

[11] W.H. Ang, I. Khalaila, C.S. Allardyce, L. Juillerat-Jeanneret, P.J. Dyson, J. Am. Chem. Soc. 127 (2005) 1382-1383.

[12] M.D. Hall, T.W. Hambley, Coord. Chem. Rev. 232 (2002) 49-67.

[13] S. Hanessian, L.J. Zhan, R. Bovey, O.M. Saavedra, L. Juillerat-Jeanneret, J. Med. Chem. 46 (2003) 3600-3611.

[14] C.F. Chin, Q. Tian, M.I. Setyawati, W. Fang, E.S.Qing Tan, D.T. Tai Leong, W.H. Ang, J Med Chem. 55 (2012) 7571-7582.

[15] W. H. Ang, S. Pilet, R. Scopelliti, F. Bussy, L. Juillerat-Jeanneret, P.J. Dyson, J. Med. Chem. 48 (2005) 8060-9.

[16] V. Gandin, C. Marzano, G. Pelosi, M. Ravera, E. Gabano, D. Osella, ChemMedChem, 6 (2014) 1299-1305.

[17] P.S. Pregosin, Coord. Chem. Rev. 44 (1982) 247-291.

[18] R. Ranaldo, N. Margiotta, F.P. Intini, C. Pacifico, G. Natile, Inorg. Chem., 47 (2008) 2820-2830.

[19] E. Petruzzella, N. Margiotta, M.Ravera, G. Natile, Inorg. Chem. 52 (2013) 2393-2403.

[20] Bruker: SAINT-IRIX. Bruker AXS, Inc.: Madison, WI, 2003.

[21] G.M. Sheldrick, SADABS, Program for Empirical Absorption Correction of Area Detector Data; University of Göttingen: Germany, 1996.

[22] M.C. Burla, M. Camalli, B. Carrozzini, G.L. Cascarano, C. Giacovazzo, G. Polidori, R. Spagna, J. Appl. Crystallogr. 36 (2003) 1103.

[23] G.M. Sheldrick, Acta Crystallogr., Sect. A: Found. Crystallogr. 64 (2008) 112−122.

[24] M. Nardelli, Comput. Chem. 7 (1983) 95−97.

[25] M. Nardelli, J. Appl. Crystallogr. 28 (1995) 659–660.

[26] L.J. Farrugia, J. Appl. Crystallogr. 32 (1999) 837−838.

[27] L.J. Farrugia, J. Appl. Crystallogr. 30 (1997) 565.

[28] V. Gandin, M. Pellei, F. Tisato, M. Porchia, C. Santini, C. Marzano, J. Cell. Mol. Med. 16 (2012) 142–151.

[29] M. Galanski, B.K. Keppler, Inorg. Chem. 35 (1996) 1709-1711.

[30] A.R. Khokhar, S. Shamsuddin, Q. Xu, Inorg. Chim. Acta. 219 (1994) 193.

[31] S. Shamsuddin, C.C. Santillan, J.L. Stark, K.H. Whitmire, Z.H. Siddik, A.R. Khokhar, Journal of Inorganic Biochemistry 71 (1998) 29-35.

[32] S. Shamsuddin, J.W. van Hal, J.L. Stark, K.H. Whitmire, A.R. Khokhar, Inorg. Chem. 36 (1997) 5969-5971.

[33] C.F. Chin, D.Y.Q. Wong, R. Jothibasu, W.H. Ang, Curr. Trends Med. Chem., 11 (2011) 2602–2612.

[34] E. Wexselblatt, D. Gibson, J. Inorg. Biochem., 117 (2012) 220–229.

[35] S. Dhar, S.J. Lippard, PNAS, 106 (2009) 22199-22204.

[36] E. Wexselblatt, E. Yavin, D. Gibson. Angew. Chem. Int. Ed. 52 (2013) 6059-6062.

[37] A.R. Khokhar, S. Al-Baker, S. Shamsuddin, Z. H.Siddik, J. Med. Chem., 40 (1997) 112–116.

Table 1. Crystal data for c*is*,*trans*,*cis*-[$PtCl_2$(benzoate)$_2$(*cis*-1,4-DACH)] (**1**).

Empirical formula	C_{20} H_{24} Cl_2 N_2 O_4 Pt
Formula weight	622.40
Temperature	293(2) K
Wavelength	0.71073 Å
Crystal system	monoclinic
Space group	C 2/c
Unit cell dimensions	a = 22.341(4) Å b = 8.5610(10) Å c = 12.831(2) Å β= 113.204(10)°.
Volume	2255.6(6) $Å^3$
Z	4
Density (calculated)	1.833 Mg/m^3
Absorption coefficient	6.485 mm^{-1}
F(000)	1208
Crystal size	0.990x0.318x0.208 mm^3
Theta range for data collection	1.98 to 23.54°.
Index ranges	-23<=h<=24, -9<=k<=9, -14<=l<=14
Reflections collected	10925
Independent reflections	1655 [R(int) = 0.0652]
Completeness to theta = 23.54°	98.5 %
Refinement method	Full-matrix least-squares on F^2
Data / restraints / parameters	1655 / 0 / 134
Goodness-of-fit on F^2	1.168
Final R indices [I>2sigma(I)]	R1 = 0.0504, wR2 = 0.1184
R indices (all data)	R1 = 0.0650, wR2 = 0.1246
Largest diff. peak and hole	1.689 and -1.127 e.$Å^{-3}$

Table 2. Selected bond lengths [Å] and angles [°] for c*is*,*trans*,*cis*-[$PtCl_2$(benzoate)$_2$(*cis*-1,4-DACH)] (**1**).

Pt(1)-O(1)#1	1.979(9)	O(1)-Pt(1)-N(1)#1	85.5(3)
Pt(1)-O(1)	1.979(9)	N(1)-Pt(1)-N(1)#1	96.8(4)
Pt(1)-N(1)	2.084(9)	O(1)#1-Pt(1)-Cl(1)	94.4(2)
Pt(1)-N(1)#1	2.084(9)	O(1)-Pt(1)-Cl(1)	85.6(2)
Pt(1)-Cl(1)	2.322(3)	N(1)-Pt(1)-Cl(1)	177.2(2)
Pt(1)-Cl(1)#1	2.322(3)	N(1)#1-Pt(1)-Cl(1)	86.1(2)
N(1)-C(8)	1.478(15)	O(1)#1-Pt(1)-Cl(1)#1	85.6(2)
O(1)-C(1)	1.326(14)	O(1)-Pt(1)-Cl(1)#1	94.4(2)
O(2)-C(1)	1.206(13)	N(1)-Pt(1)-Cl(1)#1	86.1(2)
C(1)-C(2)	1.505(18)	N(1)#1-Pt(1)-Cl(1)#1	177.2(2)
O(1)#1-Pt(1)-O(1)	179.9(5)	Cl(1)-Pt(1)-Cl(1)#1	91.06(17)
O(1)#1-Pt(1)-N(1)	85.5(3)	C(8)-N(1)-Pt(1)	124.5(6)
O(1)-Pt(1)-N(1)	94.5(3)	C(1)-O(1)-Pt(1)	126.1(7)
O(1)#1-Pt(1)-N(1)#1	94.5(3)	O(1)#1-Pt(1)-Cl(1)	94.4(2)

Symmetry transformations used to generate equivalent atoms: # -*x*+1,y,-*z*+1/2+1

Table 3. Intramolecular and intermolecular hydrogen bonds for complex c*is*,*trans*,*cis*-[$PtCl_2$(benzoate)$_2$(*cis*-1,4-DACH)] (**1**).

D—H···A	DH···A(Å)	D···A(Å)	D—H···A(°)	Symmetry codes
N1—H1a···O2	2.00(1)	2.78(1)	144(3)	
N1—H1b···O2	2.20(1)	2.92(1)	136(1)	*-x+1,-y+1,-z+2*
C10—H10a···Cl1	2.82(1)	3.74(1)	159(1)	*-x+1,+y+1,-z+1/2+1*

Table 4. *In vitro* antitumor activity.

Compound	IC_{50} (μM) ± D.S.								
	HCT-15	**BxPC3**	**A375**	**A549**	**MCF-7**	**2008**	**C13***	**LoVo**	**LoVo OXP**
1	0.07±0.05	0.03±0.02	0.06±0.04	0.05±0.01	0.08±0.02	0.09±0.03	0.06±0.01 (0.7)	0.09±0.02	0.08±0.01 (0.9)
2	0.37±0.25	0.32±0.12	0.36±0.17	0.54±0.31	0.41±0.15	0.18±0.06	0.17±0.02 (0.9)	0.31±0.92	0.51±0.11 (1.6)
3	10.32±1.42	38.87±5.48	6.23±2.96	39.76±0.81	7.07±2.05	9.42±1.8	13.85±3.53 (1.5)	6.64±2.07	9.46±2.15 (1.6)
Kiteplatin	2.66±0.95	3.93±0.84	1.87±1.25	2.01±0.77	3.09±1.06	1.89±1.04	1.77±0.92 (0.9)	1.11±0.45	1.29±0.82 (1.2)
Cisplatin	15.25±2.24	7.34±1.17	3.11±0.98	7.46±1.25	8.78±1.32	2.14±1.05	22.13±2.45 (10.3)	9.12±1.35	16.16±3.36 (1.9)

S.D.= standard deviation. Cells ($3\text{-}8\cdot10^4\cdot mL^{-1}$) were treated for 72 h with increasing concentrations of tested compounds. Cytotoxicity was assessed by MTT test. IC_{50} values were calculated by four parameter logistic model ($P < 0.05$). Data in parentheses are the resistance factors R.F. = IC_{50} (resistant subline) / IC_{50} (wild-type cells).

Figure(s)

Click here to download Figure(s): Figures.docx

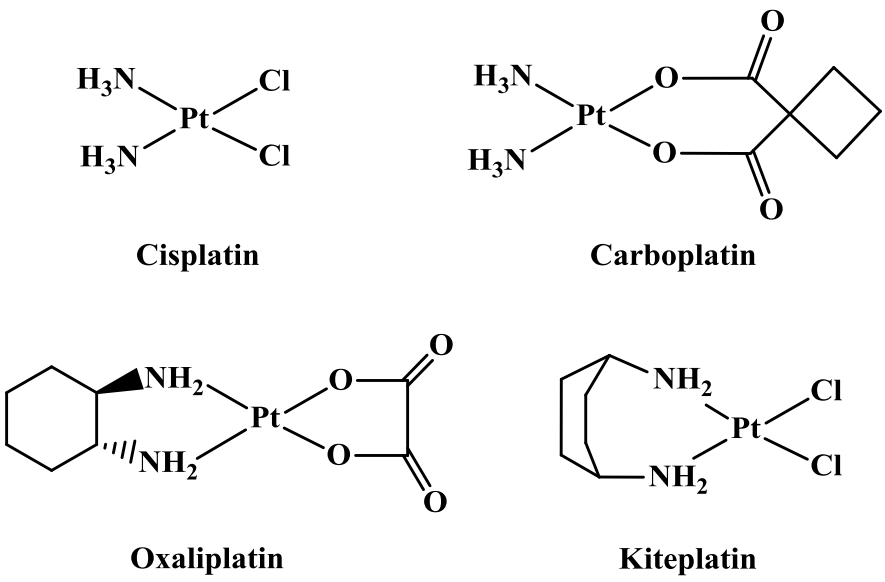

Chart 1. Pt(II) complexes.

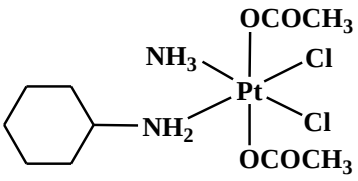

Satraplatin

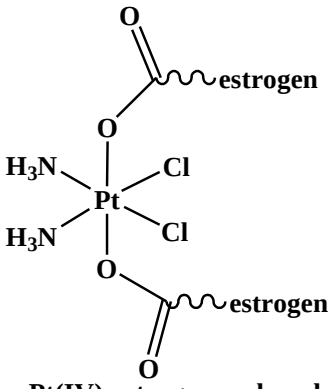

Pt(IV)-estrogen carboxylates

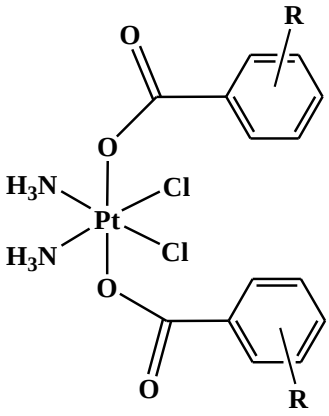

***cis,trans,cis*[$PtCl_2$(benzoate)$_2$(NH_3)$_2$]**

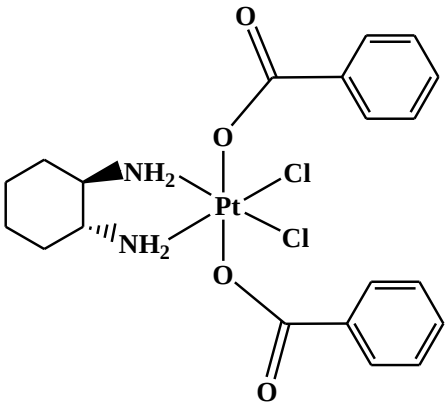

***cis,trans,cis*[$PtCl_2$(benzoate)$_2$(1*R*,2*R*-diaminocyclohexane)]**

Chart 1. Pt(IV) complexes.

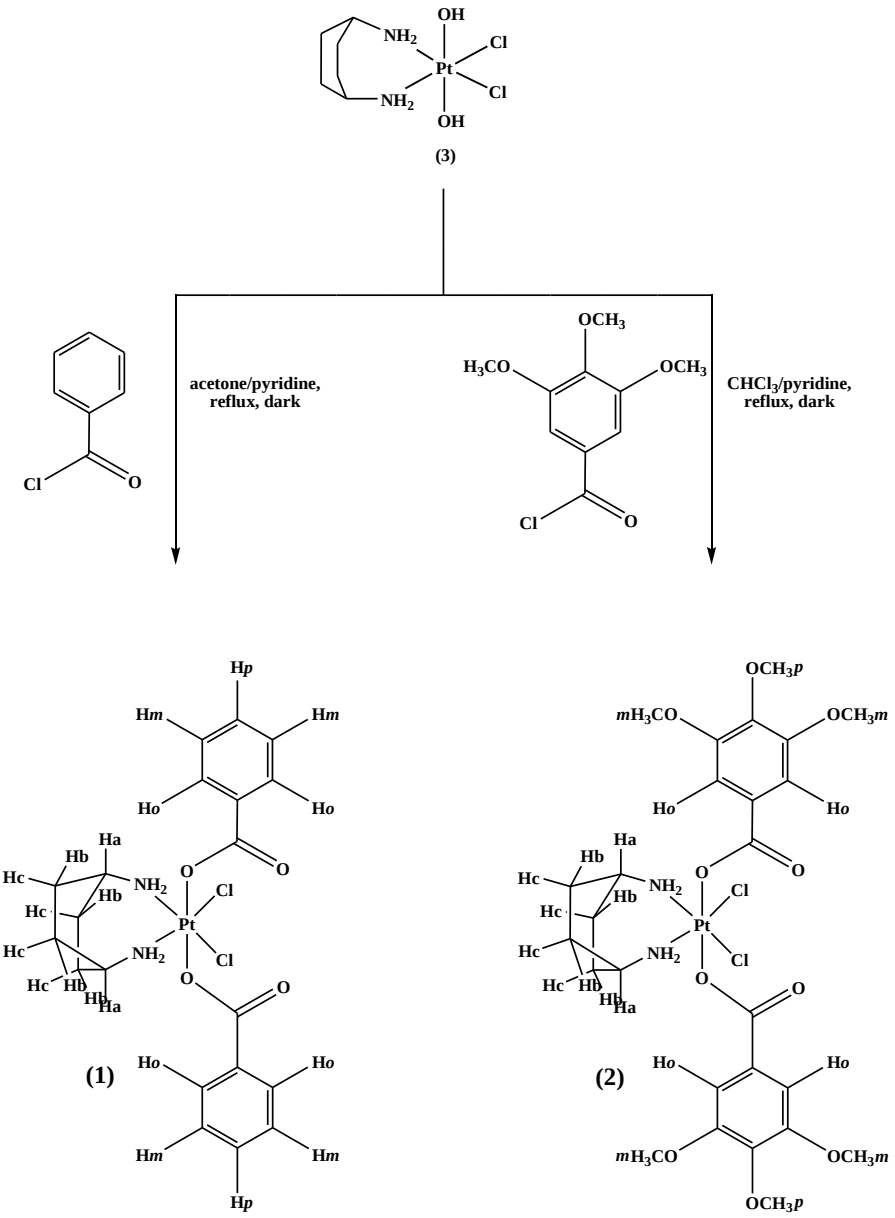

Scheme 1. Synthetic routes used to prepare the Pt(IV) aryl carboxylate complexes *cis*,*trans*,*cis*-[$PtCl_2$(benzoate)$_2$(*cis*-1,4-DACH)] (**1**) and *cis*,*trans*,*cis*-[$PtCl_2$(3,4,5-trimethoxybenzoate)$_2$(*cis*-1,4-DACH)] (**2**).

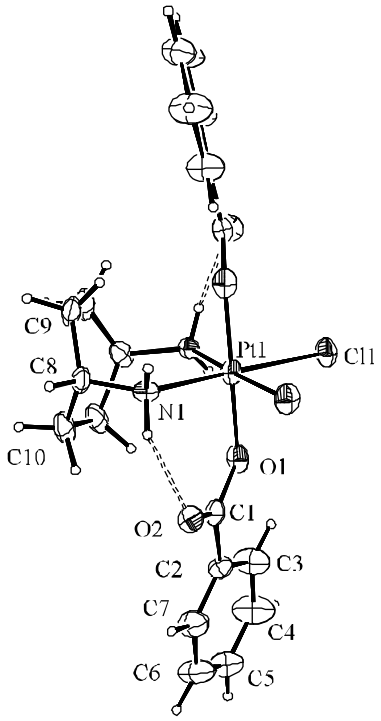

Figure 1. ORTEP view of **1** with atom numbering scheme. Displacement ellipsoids are represented at 20% probability levels. Intramolecular hydrogen bonds are shown as dashed lines.

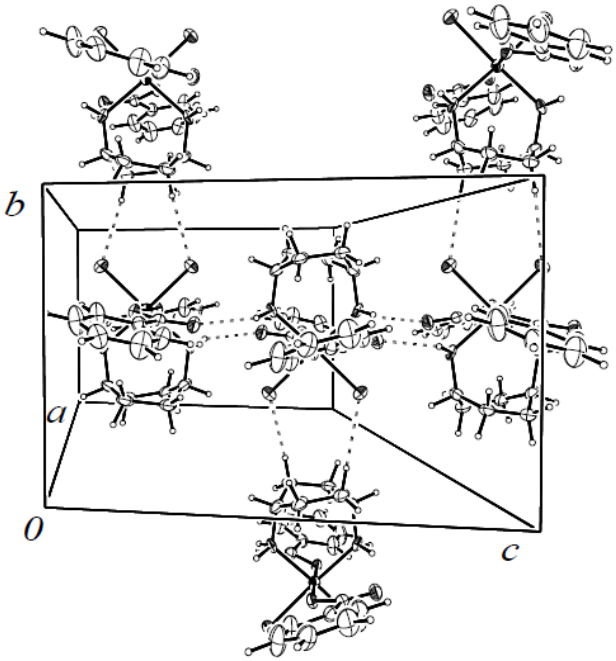

Figure 2. Crystal packing of **1** showing the web of hydrogen-bonding.

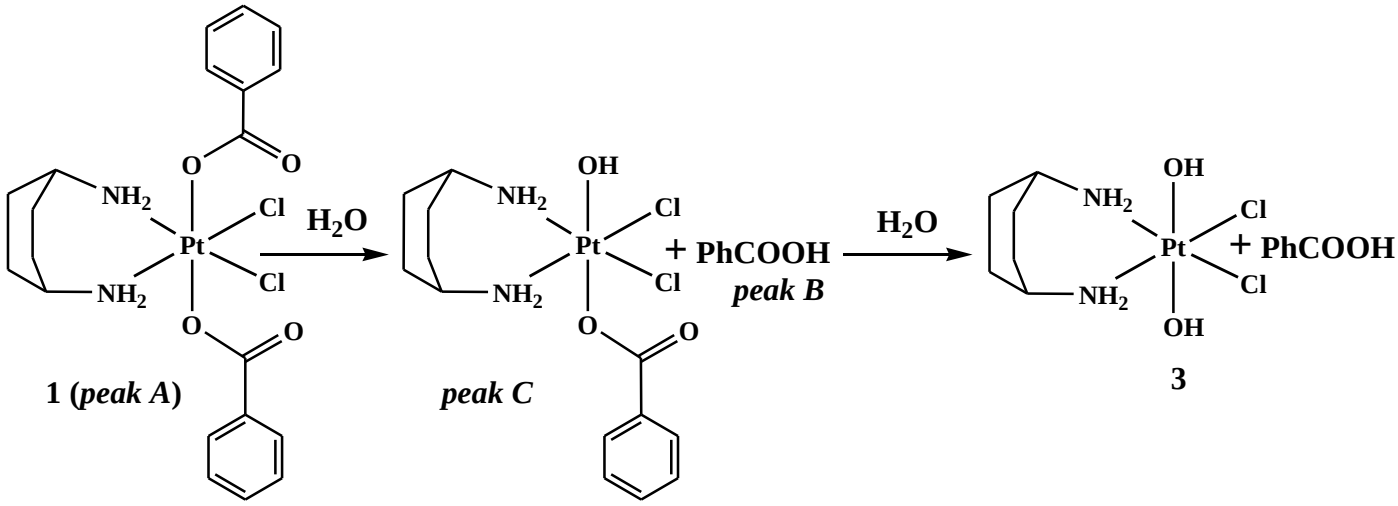

Scheme 2. Description of possible metabolites formed by **1** in solution. In parentheses are indicated the corresponding peaks shown in the chromatograms of Figure 3.

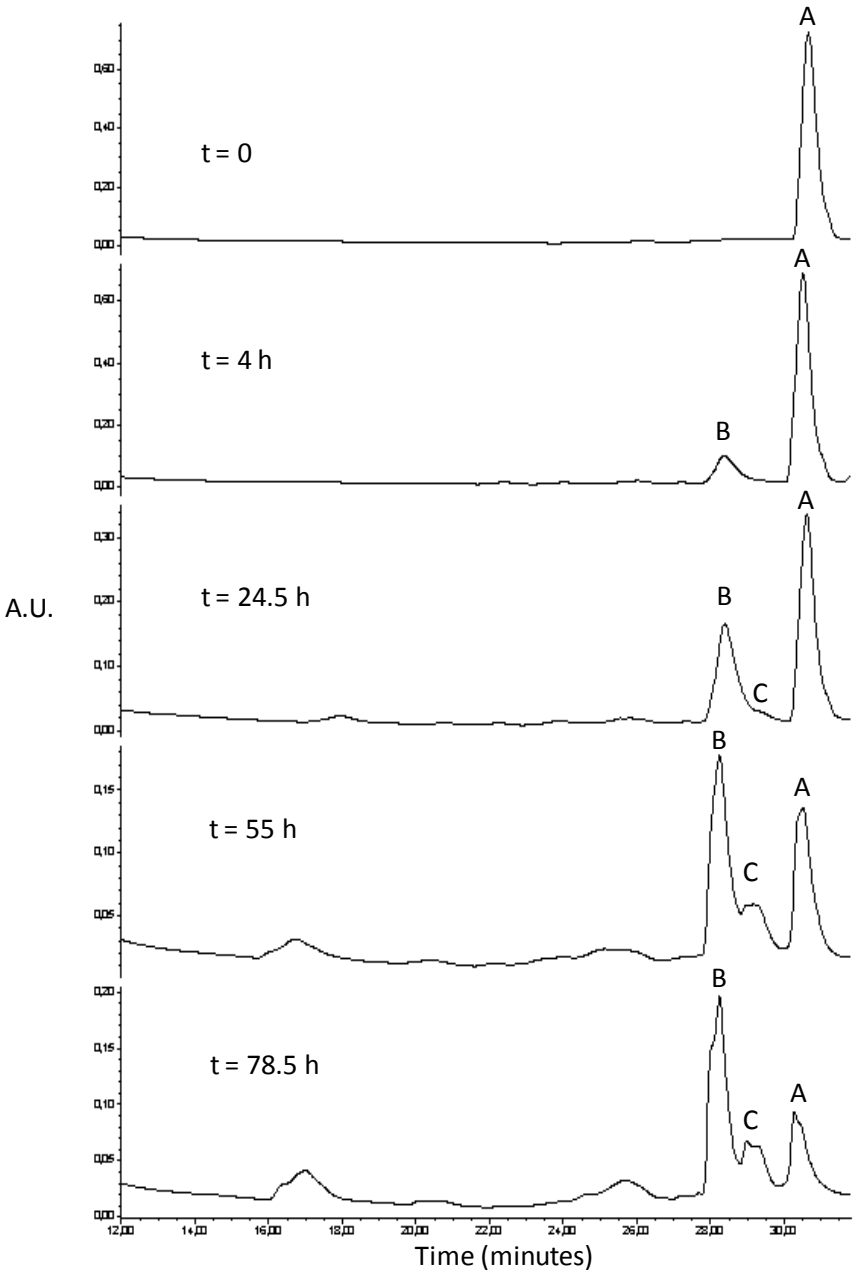

Figure 3. HPLC chromatograms at different times of incubation of complex **1** in DMSO/saline (5:95, V/V; pH = 6.2; T = 37 °C), (A = complex **1**, B = benzoic acid, C = *cis*,*trans*,*cis*-[$PtCl_2$(benzoate)(OH)(*cis*-1,4-DACH)]).

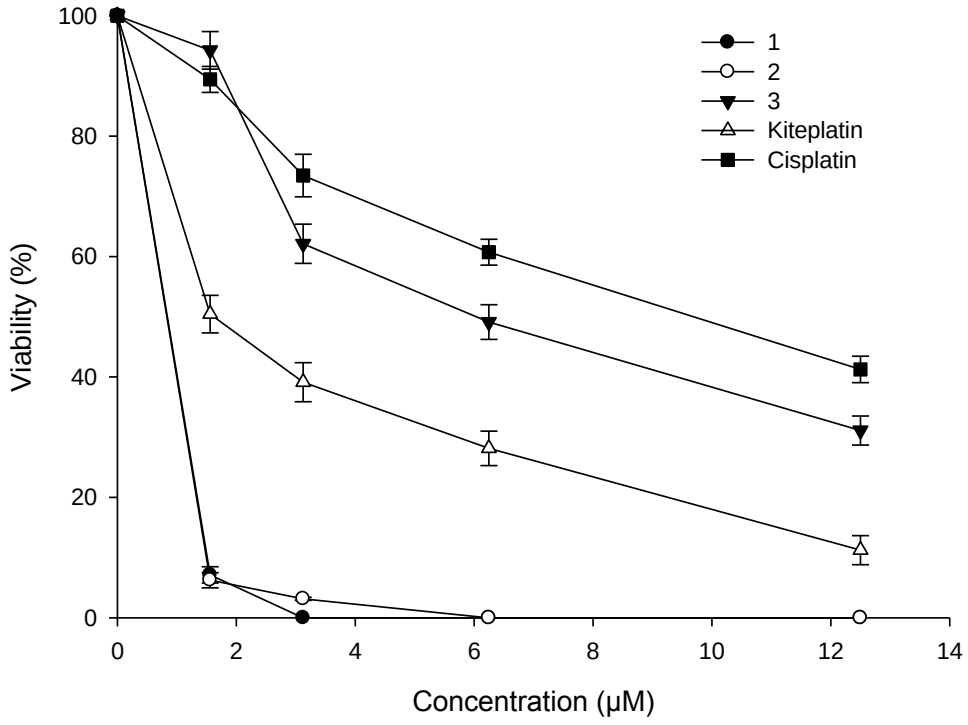

Figure 4. Cell growth recovery: cells were treated for 6 h with the indicated compounds, washed, and re-incubated with fresh complete medium for further 66 h before MTT determination. Data are the means of three independent experiments. Error bars indicate SD**.**

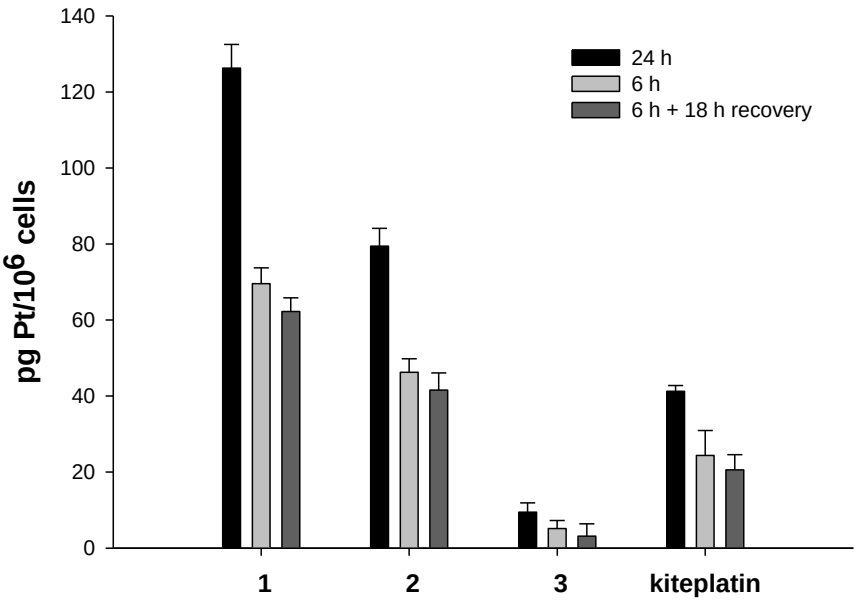

Figure 5. Intracellular accumulation induced by compounds **1, 2** and **3** as well as kiteplatin. LoVo cells were incubated with 1 μM of tested complexes for 6 or 24 h. In cell recovery experiments, cells were treated with 1 μM of tested complexes for 6 h, washed and re-incubated for additional 18 h in fresh medium. The Pt cellular content was estimated by means of GF-AAS analysis. Data are the means of three independent experiments. Error bars indicate SD**.**

Supplementary Information for Publication Online

Click here to download Supplementary Information for Publication Online: margiotta_metallodrugs_SUP_INFO.pdf

CIF File(s) (REQUIRED if paper describes X-ray crystal structures)

Click here to download CIF File(s) (REQUIRED if paper describes X-ray crystal structures): CCDC_1426597.CIF

CIF Validation Report(s) (RECOMMENDED if paper describes X-ray crystal structures)

Click here to download CIF Validation Report(s) (RECOMMENDED if paper describes X-ray crystal structures): checkcif.pdf